Carbohydrate Polymers 115 (2015) 516–524

Contents lists available at ScienceDirect

Carbohydrate Polymers

journal homepage: www.elsevier.com/locate/carbpol

Formation of self-extinguishing flame retardant biobased coating on cotton fabrics via Layer-by-Layer assembly of chitin derivatives

Haifeng Pan[a,b], Wei Wang[a], Ying Pan[a], Lei Song[a,*], Yuan Hu[a,b,**], Kim Meow Liew[b,c]

[a] State Key Laboratory of Fire Science, University of Science and Technology of China, 96 Jinzhai Road, Hefei, Anhui 230026, People's Republic of China
[b] Suzhou Key Laboratory of Urban Public Safety, Suzhou Institute of University of Science and Technology of China, 166 Ren'ai Road, Suzhou, Jiangsu 215123, People's Republic of China
[c] Department of Building and Construction, City University of Hong Kong, Tat Chee Avenue, Kowloon, Hong Kong

ARTICLE INFO

Article history:
Received 19 May 2014
Received in revised form 15 August 2014
Accepted 17 August 2014
Available online 2 September 2014

Keywords:
Self-extinguishing
Phosphorylated chitin
Chitosan
Layer-by-Layer assembly method

ABSTRACT

The self-extinguishing coating, consisting of biobased chitin derivatives, phosphorylated chitin and deacetylated chitin (chitosan), was deposited on cotton fabrics via the Layer-by-Layer (LbL) assembled method. The content of phosphorylated chitin prepared on cotton fabrics surface is dependent on the bilayers' number and concentration of phosphorylated chitin. In the vertical flame test, the cotton fabric with 20 bilayers prepared at the high phosphorylated chitin concentration (2 wt%) could extinguish the flame. Microcombustion calorimetry result showed that all coated cotton fabrics showed lower peak heat-release rate and total heat-release values compared with that of the pure one. Thermogravimetric analysis result indicated that thermal and thermal oxidation stability of all coated cotton fabrics were enhanced in the high temperature range (400–700 °C). This work provided the flame retardant multilayer films based on fully biobased chitin derivatives on cotton fabrics to enhance its flame retardancy.

1. Introduction

Polysaccharides are a family of carbohydrates that play fundamental roles in many biological contexts. Their structure is made of sugar rings linked by glycosidic bonds and various side functions. Chitin, the second most abundant polysaccharide, occurs in nature as ordered microfibrils and is the major structural component in the exoskeleton of arthropods and cell walls of fungi and yeast. It is a linear cationic heteropolymer of randomly distributed *N*-acetyl glucosamine and glucosamine residues with β-1,4-linkage. Chitobiose, 4-*O*-(2-amino-2-deoxy-β-D-glucopyranosyl) -(1→4)-2-amino-2-deoxy-D-glucose, is the structural unit of native chitin (Yui, Kobayashi, Kitamura, & Imada, 1994). Chitin has emerged as a new class of physiological materials due to its versatile biological activity, excellent biocompatibility and complete biodegradability in combination with low toxicity (Marguerite, 2006). It is also an interesting polysaccharide because of the presence of an amino functionality and two hydroxyl functionalities, which could be suitable for chemical modification. As with cellulose, chitin can undergo many reactions such as etherification (Gorochovceva and Makusuka, 2004; Kurita, 2001; Zhang and Ren, 2007), esterification (Yoshifuji, Noishiki, Wada, Heux, & Kuga, 2006), graft copolymerization (Jayakumar, Prabaharan, Reis, & Mano, 2005), etc. After the chemical modification, chitin would bring new properties depending on the nature of the group introduced. Recently, phosphorylated chitin is widely reported owing to its interesting biological and chemical properties: biocompatible (Wang, Ma, Wang, & He, 2002; Wang, Ma, Feng, & Cui, 2002; Wang, Zhu, Feng, Cui, & Ma, 2003), bioabsorbable (Wang, Ma, Wang et al., 2002; Wang, Ma, Feng et al., 2002; Yokogawa et al., 1997) and metal chelating properties. Phosphorylated chitin could be the anionic polyelectrolyte owing to the phosphate group introduced. Additionally, phosphorylated chitin could show the flame retardant property due to the introduction of flame retardant phosphorus element. Chitosan that composed of residues of glucosamine and *N*-acetyl glucosamine connected via a–b (1–4) linkage is the deacetylated derivatives of chitin. Chitosan is expected to act as a char-forming agent owing to the structure of polyhydroxy and could also be a blowing agent, releasing ammonia as it degrades.

It is simple and versatile to incorporate various polymers, colloids or molecules into a thin film via the Layer-by-Layer assembled method. Recently, the extensive application of the LbL assembly technique in improving the flame retardancy of

* Corresponding author. Tel.: +86 551 63601664; fax: +86 551 63601664.
** Corresponding author at: State Key Laboratory of Fire Science, University of Science and Technology of China, 96 Jinzhai Road, Hefei, Anhui 230026, People's Republic of China. Tel.: +86 551 63601664; fax: +86 551 63601664.
E-mail addresses: leisong@ustc.edu.cn (L. Song), yuanhu@ustc.edu.cn (Y. Hu).

http://dx.doi.org/10.1016/j.carbpol.2014.08.084
0144-8617/

substrate was widely reported. Grunlan and co-workers firstly used the Layer-by-Layer assembled thin films comprised of branched polyethylenimine and Laponite clay platelets to improve flame retardancy of cotton fabric (Li, Schulz, & Grunlan, 2009). Then, many nanoparticles and polyelectrolytes have been successively used as Layer-by-Layer assembled films to deposit on cotton fabric or other fabrics (Alongi, Carosio, & Malucelli, 2012; Carosio, Alongi, & Malucelli, 2011; Carosio, Laufer, Alongi, Camino, & Grunlan, 2011; Carosio, Alongia, & Malucelli, 2012; Carosio, Blasio, Alongi, & Malucelli, 2013; Laufer, Carosio, Martinez, Camino, & Grunlan, 2011; Laufer, Kirkland, Morgan, & Grunlan, 2012; Li, Mannen, Schulz, & Grunlan, 2011; Li, Mannen, Morgan, Chang, & Yang, 2011). Many synthetic polyelectrolytes, such as polyethylenimine (PEI), polyallylamine (PAH) and polyacrylic acid (PAA), have been widely used as polyelectrolytes multilayer (PEM) films for Layer-by-Layer assembly. The polysaccharide-based PEM films have also attracted considerable attention due to the interest in green chemistry and concern over toxicity and environmental issues in the recent years. Recently, chitosan was used as cationic part of PEM films to impart the flame retardancy to PET fabric and cotton fabric (Carosio et al., 2012; Laufer et al., 2011). Furthermore, the green nanocoating based on chitosan/phytic acid and chitosan/DNA bilayers were also studied to antiflammable treatment for cotton fabric (Carosio et al., 2013; Laufer et al., 2012). Among these films, chitosan generally acted as a char-forming agent and foaming agent. Recently, our research group has successfully prepared some phosphorylated polysaccharides, which show effective flame retardancy for polymeric materials (Hu, Song, Pan, Hu, & Gong, 2012; Hu, Song, Pan, & Hu, 2012; Hu, Song, Pan, & Hu, 2013). Phosphorylated polysaccharides can show flame retardancy owing to the flame retardant intumescent-like system, in which polyhydroxy structure of sugar units could act as carbon source and phosphate group could act as acidic source. In our present study, a biobased flame retardant PEM film consisting of fully chitin derivatives was deposited on the surface of cotton fabric to reduce its flammability. Flame retardant properties of uncoated and coated cotton fabrics were studied by vertical flame test and microcombustion calorimetry (MCC). The thermal properties were investigated by the thermogravimetric analysis (TGA), real-time Fourier transform infrared (RT-IR) and thermogravimetric analysis/infrared spectrometry (TGA-IR).

2. Experiment

2.1. Materials

Chitin was purchased from ShangHai Guoyao Chemical Company. Chitosan (viscosity 50–800 mPa s, degree of deacetylation 80–95%), phosphorus pentoxide and methanesulfonic acid were all provided by Sinopharm Chemical Reagent Co., Ltd. Deionized water with a resistance of 18.2 MΩ was used for all experiments. Cotton fabric was supplied by Jiangxi JingZhu Ramie Textile Co.

3. Preparation of phosphorylated chitin

Phosphorylated chitin (PT) was prepared by the reaction with phosphorus pentoxide in methanesulfonic acid solution according to the procedure mentioned by Nishi et al. (1986). Briefly, chitin (2 g) and methanesulfonic acid (30 mL) were placed into a three-necked flask with a mechanical stirrer. The flask was put in an ice bath with N_2 gas that was aspirated to eliminate residual moisture. Phosphorus pentoxide (10 g) was added and the reaction went on for 3 h in ice bath. The product was washed with ether, acetone, methanol and ether for three times. Then, the product was further purified by diafiltration overnight. As a result, the PT solution could be obtained.

4. Layer-by-Layer deposition for cotton fabrics

Phosphorylated chitin (PT) solution (anionic deposition solutions) at pH 7 was prepared by adjusting pH values of deionized (DI) water (18.2 MΩ) with 1 M hydrochloric acid (HCl) or 1 M sodium hydroxide solution. The concentrations were 0.5 wt% and 2 wt%, respectively. In addition, chitosan solution (cationic deposition solutions) was prepared as 0.5 wt% concentration using deionized water and the pH was adjusted to 4 with 1 M HCl solution. Prior to the deposition, cotton fabrics were washed with distilled water, and then air-dried at room temperature overnight. Substrates were alternately dipped into cationic and anionic solutions. Cotton fabric was initially dipped in the cationic chitosan solution for 5 min, subsequent dips were 1 min in the anionic PT solution. Each dip was followed by rinsing with DI water and wringed out by hand to expel liquid among cotton fabrics. After the desired number of bilayers was deposited, cotton fabrics were dried at 70 °C overnight before testing. The weight gain for cotton fabric was calculated from the mass measured before and after coating using a laboratory microbalance. The Layer-by-Layer assembly process was shown in Scheme 1. In this work, we denote briefly the coated cotton fabric that was assembled in chitosan solution at a concentration of 0.5 wt% and PT solution at a concentration of 2 wt% for 20 bilayers as $(CH0.5/PT2)_{20}$.

5. Measurements

FTIR spectra were recorded on a Nicolet MAGNA-IR 750 FTIR spectrometer. KBr was ground in a mortar with a pestle, and enough solid sample was ground with KBr to make a 1 wt% mixture for making KBr pellets. The mixture was pressed into a tablet, which was then placed in a ventilated oven. The transition mode was used and the wavelength range was set from 4000 to 500 cm^{-1}. Atomic absorption spectrometry (Analyst 800, Perkin-Elmer) was used to test the phosphorus content of phosphorylated chitin. Attenuated total reflection Fourier transform infrared (ATR-FTIR) spectra, in the frequency region of 4000 – 400 cm^{-1} at a 4 cm^{-1} resolution, were recorded by a Nicolet 6700 spectrometer (Thermo-Nicolet) using 32 scans. Thermogravimetric analysis (TGA) of samples was examined on a TGA-Q5000 apparatus (TACompany, USA) from 50 to 600 °C at a heating rate of 20 °C/min. The weight of all samples was kept within 3–5 mg in an open Alumina pan. Vertical flame tests were performed according to ASTM D6413-08, using a vertical burning tester (CZF-3, Nanjing Jiangning Analytical Instrument Factory, China). The samples (300 mm × 76 mm), held 19 mm over the Bunsen burner, were first exposed to the flame for a period of 12 s and then removed rapidly. Heat release rate (HRR) and total heat release (THR) were measured in a microscale combustion calorimeter (GOVMARK MCC-2). About 5 mg samples were heated at a heating rate of 1 K/s in a nitrogen stream flowing at 80 cm^3/min. The degradation products of the sample in nitrogen atmosphere were mixed with a 20 cm^3/min stream of pure oxygen prior to entering a 900 °C combustion furnace. Real-time Fourier transform infrared (RT-IR) method used a Nicolet MAGNA-IR 750 spectrophotometer (Nicolet Instrument Company, USA) to study the thermo-oxidative degradation of pure and coated cotton fabrics. Powders of the cured sample were mixed with KBr powders, and the mixture was pressed into a tablet, which was then placed into the oven. The temperature of the oven was raised at a heating rate of about 10 °C/min. Thermogravimetric analysis/infrared spectrometry (TG-IR) of the samples was performed using the TGA Q5000IR thermogravimetric analyzer that was interfaced to the Nicolet 6700 FTIR spectrophotometer. About 5.0 mg of the sample was put in an alumina crucible and heated from 30 to 600 °C at a heating rate of 20 °C/min (nitrogen atmosphere, flow rate of 45 mL/min). The morphologies of pure

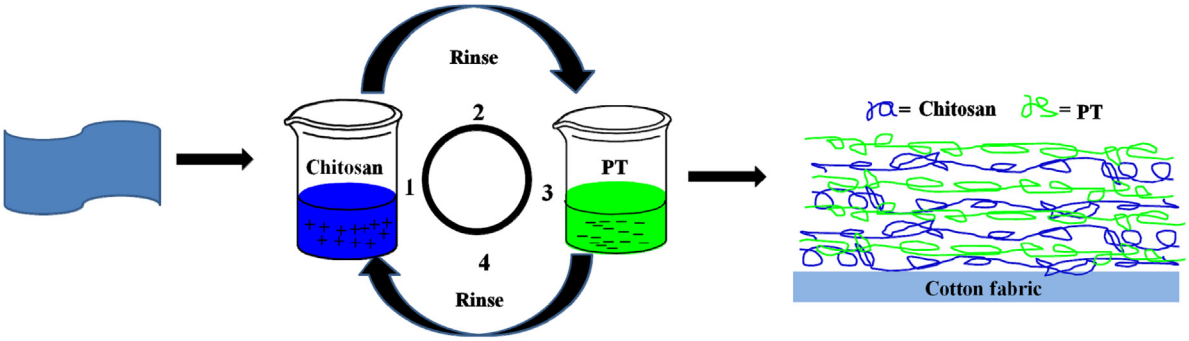

Scheme 1. The scheme of layer by layer assembly using chitosan (CH) and phosphorylated chitin (PT).

and coated cotton fabrics, along with the char residues after vertical flame tests, coated with a gold layer in advance were observed using scanning electron microscopy with an energy-dispersive X-ray (EDX) analyzer. (SEM, AMRAY1000B, Beijing R&D Center of the Chinese Academy of sciences, China).

6. Results and discussion

6.1. Chemical structural analysis of chitin and phosphorylated chitn (PT)

Fig. 1A shows the FTIR spectra of chitin and phosphorylated chitin (PT). Typically, in the FTIR spectrum of chitin, the following characteristic bands can be observed: the bands at 3400–3300 cm^{-1} could be attributed to the stretching vibration of OH group at the sugar unit; the bands at 2870–2970 cm^{-1} is attributing to CH_2 groups. Peaks at 1160 and 1110 cm^{-1} are corresponding to the stretching vibration of C—O—C from the glucosidic units or from β-(1→4)-glucosidic bonds; peaks at 1640 and 1560 cm^{-1} are corresponding to the stretching vibration of C=O and N—H, respectively, indicating the amide group from the sugar unit (Kim, Kim, & Lee, 1996). In the FTIR spectra of phosphorylated chitin (PT), two new characteristic peaks appear at 1040 cm^{-1} and 490 cm^{-1}, which can be attributed to the P—O structure, such as P—O—C and P—OH. The peak at 1040 cm^{-1} overlaps the C—O stretching vibrations in chitin ether groups at 1100 cm^{-1} (Jayakumar, Egawa, Furuike, Nair, & Tamura, 2009). In addition, atomic absorption spectrometry reveals that the content of phosphorus in PT is 12.5%.

7. Characterization of (CH/PT) coated cotton fabrics

Surface chemical structures of cotton fabrics can be qualitatively determined by ATR-FTIR spectroscopy. ATR-FTIR is an IR sampling technique and can measure the changes in an infrared beam with totally internal reflection when it comes into contact with the surface of samples. The ATR-FTIR spectra of pure and (CH0.5/PT0.5) coated cotton fabrics are shown in Fig. 1B as representatives to monitor the growth of bilayers on the surface of cotton fabrics. Compared with pure cotton fabric, the ATR-FTIR spectra of (CH0.5/PT0.5) coated samples appear two new peaks (1640 $cm^{-1}$and 1560 cm^{-1}), which are ascribed to the stretching vibration of amide group for phosphorylated chitin (PT). Furthermore, the intensity of the two peaks' absorbance increase obviously as the bilayers' number increase, indicating that PT have been gradually incorporated into the polyelectrolyte multilayer (PEM) films during the deposition. However, the similar phenomenon is not observed for the peaks at 1040 cm^{-1} (stretching vibration of P—O—C), which can be ascribed to the overlap of the vibration of C—O—C (1046 cm^{-1}) from cellulose molecular chain (chemical composition of cotton fabric) (Jayakumar et al., 2009).

Energy-dispersive X-ray (EDX) is used here to confirm the key information concerning the element composition of samples. EDX spectra of pure and (CH0.5/PT0.5) coated cotton fabrics are shown in Fig. 1D as a representation to monitor the element composition of samples. It obviously shows that P element is only detected in the coated cotton fabrics, indicating the presence of phosphorylated chitin (PT) in the PEM films. Interestingly, as the number of deposition cycles is increased to 20, the P/C and P/O ratios are clearly increased, indicating the reproducible coverage of PT on the sidewall of cellulose fibers. On the other hand, the corresponding surface morphology of pure and coated cotton fabrics is shown in Fig. 1C. Pure cotton fabric shows a smooth and clean surface and the LbL coating conformally coated each individual fiber for all coated cotton fabrics. However, there are also some differences. The 5 and 10 (CH0.5/PT2) BL coated samples look very similar in terms of fiber structure and shape. When the BL number increases to 20, the thin coating can be obviously observed around the fibers. Especially for $(CH0.5/PT2)_{20}$ sample, some fibers appear linked together and the gaps between fibers gradually disappear (Li et al., 2011; Li et al. 2011a, 2011b). From the SEM images, it indirectly indicates that the thin coating is deposited on fibers via Layer-by-Layer assembled style.

The weight gain of coating mass on the surface of cotton fabric as a function of bilayers' number and concentration of PT can be shown in Table 1. The weight gain was increased with the increases of the bilayers's number and concentration of PT, indicating that the content of PT prepared on cotton fabrics surface is dependent on the bilayers's number and concentration of PT.

8. Thermal stability

TGA provides direct information about thermal degradation and thermal oxidation degradation mechanism by measuring weight loss of sample as a function of temperature. The experimental TGA and DTG curves of pure and (CH/PT) coated cotton fabrics under nitrogen atmosphere are shown in Fig. 2A and B. The initial degradation temperature (when the weight loss is 10 wt%) of samples, the mid-point temperature of the degradation ($T_{-50\%}$), the maximum weight loss temperature (T_{max}) and the char residue left at 600 °C can be observed from TGA curves. The related data are shown in table S1. All (CH/PT) coated cotton fabrics show a lower initial degradation temperature than that of the pure cotton fabric, which is mostly due to the earlier degradation of PT. However, all (CH/PT) coated cotton fabrics exhibit much high thermal stability in temperatures ranging from 400 to 600 °C, indicating the protective char formation provided by the intumescent coating at high temperature (Ma et al., 2007; Yang, Wang, Lei, Fei, & Xin, 2012). For (CH0.5/PT2) coated system, samples have higher char residue at the same bilayers number relative to (CH0.5/PT0.5) systems. For example, the char residue of $(CH0.5/PT2)_{20}$ sample at 600 °C is

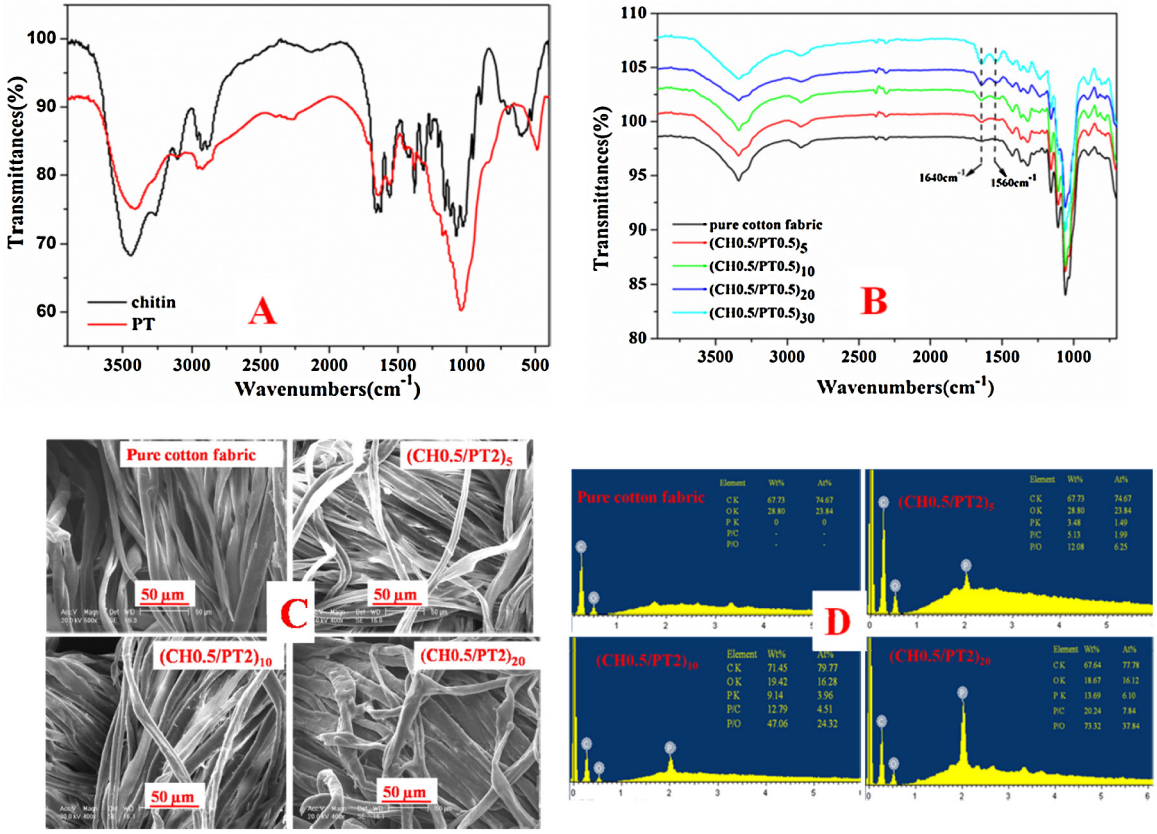

Fig. 1. (A) FTIR spectrum of chitin and phosphorylated chitin (PT); (B) ATR-FTIR spectra of pure and (CH0.5/PT0.5) coated cotton fabrics; SEM images (C) and EDX spectra (D) of pure and (CH0.5/PT2) coated cotton fabrics.

37.2%, which is higher than that (29.7%) of $(CH0.5/PT0.5)_{20}$ sample. A higher concentration of PT (2 wt%) can result in more content of PT during each deposition step than the dilute mixture (0.5 wt % PT). Hence, the result highlights the importance of the coating weight added to the cotton fabric even giving the self-extinguishing property ($(CH0.5/PT2)_{20}$ sample) during combustion by the controlling the PT concentration.

Fig. 2C and D shows the TGA and DTG curves of pure and (CH/PT) coated cotton fabrics under air atmosphere. Unlike under nitrogen atmosphere, the pure cotton fabric decomposition occurred in two main steps in air. The first region around 380 °C is the main pyrolysis region, which shows significant degradation weight loss. And it is attributed to the dehydration and decarboxylation reactions, which produce combustible gasses like aldehydes, ketones, ethers, etc (Gaan, Rupper, & Salimova, 2009; Shafizadeh & Fu, 1973). The second region around 450 °C is attributed to the further decomposition of residual char formed in the first region, which can result in the release of CO and CO_2 (Price, Horrocks, & Akalin, 1997). The pyrolysis of the coated cotton fabrics also shows two stages, but the initial decomposition temperatures generally decrease. Such an early thermal degradation is mainly ascribed to facile catalytic dehydration and cross-linking of cotton fabrics by phosphoric acid generated during pyrolysis of phosphorus-containing compounds (PT) (Kandola, Horrocks, & Price, 1996; Giraud, Bourbigot, & Rochery, 2002; Horrocks, Wang, & Hall, 2000). The coated cotton fabrics show higher solid char in the high temperature range (350–600 °C). Such improved thermal oxidation stability in the second stage is most likely due to the formation of stable intumescent chars in the first stage, which can efficiently retard the diffusion of the oxygen and heat into underlying matrix (Horrocks, Kandola, & Davies, 2005). In addition, the char residue in air for coated cotton fabrics is also dependent on the bilayers' number and concentration of PT (can be seen in Table S1).

As a result, the thermal and thermal oxidation stability are both enhanced for cotton fabric coated with (CH/PT) bilayers.

9. Flammability properties

It is necessary to test both the ignitability and the combustion behavior of pure and coated cotton fabrics in the presence of flame

Table 1
MCC data and vertical flame test data for pure and (CH/PT) coated cotton fabrics.

NUM	BL (% weight gain)	Burning time (s)	After glow time (s)	Char length (cm)	Char residue (%)	PHRR (w/g)	Temperature (°C)	THR (kJ/g)
Cotton fabric	0	7	8	30	0	204 ± 6.1	386.0 ± 7.0	8.7 ± 0.26
$(CH0.5/PT0.5)_5$	4.7	6	0	30	6.2	173 ± ± 5.2	344.0 ± 6.0	5.1 ± 0.15
$(CH0.5/PT0.5)_{10}$	9.2	5	0	30	11.5	129 ± 3.8	331.0 ± 5.8	3.8 ± 0.11
$(CH0.5/PT0.5)_{20}$	14.5	3	0	30	22.9	92.8 ± 2.7	320.0 ± 5.0	2.2 ± 0.060
$(CH0.5/PT2)_5$	8.5	4	0	30	13.8	124 ± 3.5	322.0 ± 4.2	3.2 ± 0.090
$(CH0.5/PT2)_{10}$	13.5	3	0	30	21.7	105 ± 3.1	312.0 ± 3.8	2.0 ± 0.056
$(CH0.5/PT2)_{20}$	20.5	0	0	12.5	95.2.	53.0 ± 1.6	296.0 ± 3.0	1.2 ± 0.006

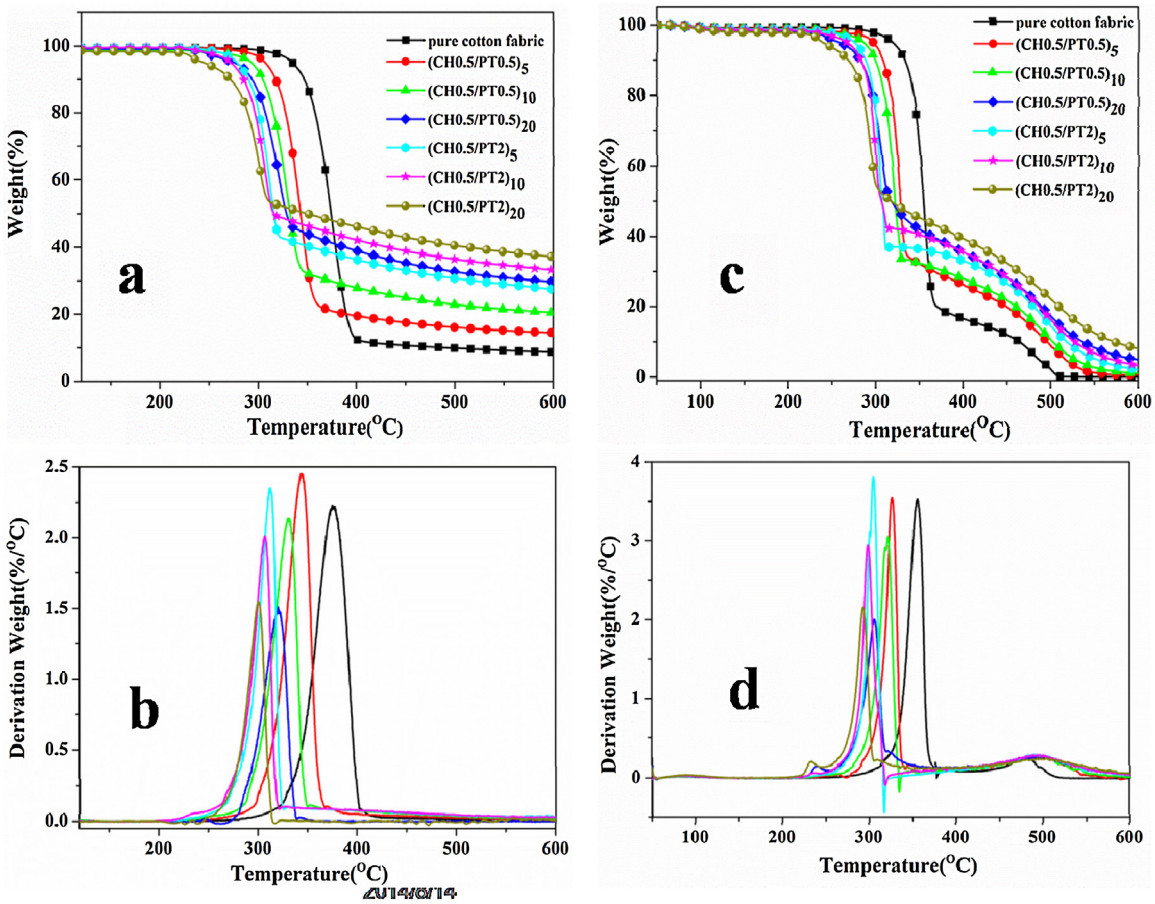

Fig. 2. TGA and DTG curves of pure and (CH/PT) coated cotton fabrics: (A, B) in nitrogen and (C, D) in air.

spread. Fig. 3A shows real-time images of vertical flame tests for pristine cotton fabric, $(CH0.5/PT0.5)_{20}$ sample and $(CH0.5/PT2)_{20}$ sample. The images of 6 s after ignition, 3 s after removal of the burner and collected char residues are treated as represents to study. For pure cotton fabric, the flame is very vigorous and spreads upward rapidly and the afterglow is obviously seen on the side 3 s after removing the burner. There is no char left for pure cotton fabric after the vertical flame test. When the $(CH0.5/PT0.5)_{20}$ sample is exposed to the same flame, the cotton fabric is consumed by the flame relatively slowly and the afterglow is disappeared. The collected char residue is integral nearly with little slits on the bottom side. As for the $(CH0.5/PT2)_{20}$ sample, the flame is not burning for 6 s after ignition and self-extinguished phenomenon can be observed, indicating that the char is durable enough to prevent additional cotton decomposition and pyrolysis and starve the flame of fuel (Li et al., 2011; Li et al. 2011a, 2011b). Flammability data are collected in Table 1. From an overall point of view, it can be shown that the (CH/PT) coated samples show some changes in the presence of Layer-by-Layer assembled coating. Pure cotton fabric is completely consumed and no char residue left during the test. In addition, afterflame time and afterglow time are 7 s and 8 s, respectively. As for all (CH/PT) coated samples, afterflame time is reduced and afterglow is eliminated. Furthermore, all coated cotton fabrics show higher char residue than that of pure cotton fabric, which can be ascribed to the dehydration and char formation of PT during burning. $(CH0.5/PT2)_{20}$ sample has the highest char residue (95.2%) owing to its self-extinguishing phenomenon. The char length of coated samples is yet the same to that of pure one except $(CH0.5/PT2)_{20}$ sample. It should be noted that burn time and afterglow time for $(CH0.5/PT2)_{20}$ sample are all eliminated and the char length is 12.5 cm, which is less than that of all other samples. The reason maybe that a higher concentration of PT (2 wt%) can result in more content of PT on cotton fabric (Li et al., 2010; Zhang et al., 2013; Zhang, Yan, Wang, & Fang, 2013). Moreover, enough amount of phosphorus content can give cotton fabric highly effective flame retardancy (Gaan & Sun, 2007). The collected char residue images of all samples are shown in Fig. 3B. The char residue of coated samples at the higher concentration (2%) is denser and thicker. Additionally, those images are consistent with the flammability data in Table 1.

Microscale combustion calorimetry (MCC) is an effective approach to obtain the information regarding combustibility and fire hazard of materials. It can quickly and easily measure the key fire parameters from just a few milligrams of specimen in minutes. Fig. 3C and D shows heat release rate (HRR) and total heat release (THR) curves of all samples. The associated data are shown in Table 1. It appears that all (CH/PT) coated cotton fabrics have lower PHRR, THR and T_{max} values compared with pure one. This may be caused by the catalytic action of phosphorus compounds, which enables cotton fabrics to dehydrate at lower temperature, and accelerates the formation of char and reduces the release of combustible gas. The lower THR values further indicate phosphorus containing PEM films could reduce fire risk of cotton fabric. Furthermore, it is clearly shown that the higher bilayers' number is, the lower combustion rate is. There is a greater reduction in THR and PHRR values for (CH0.5/PT2) coated samples, just as shown in Table 1. Its PHRR and THR values is 60.4 w/g and 1.2 KJ/g, respectively, which show 144.1 w/g and 7.5 KJ/g lower than those of pure cotton fabric. The phosphorus containing Layer-by-Layer assembled coating accelerates formation of char residue, indicating that more volatile products were catalytically carbonized to

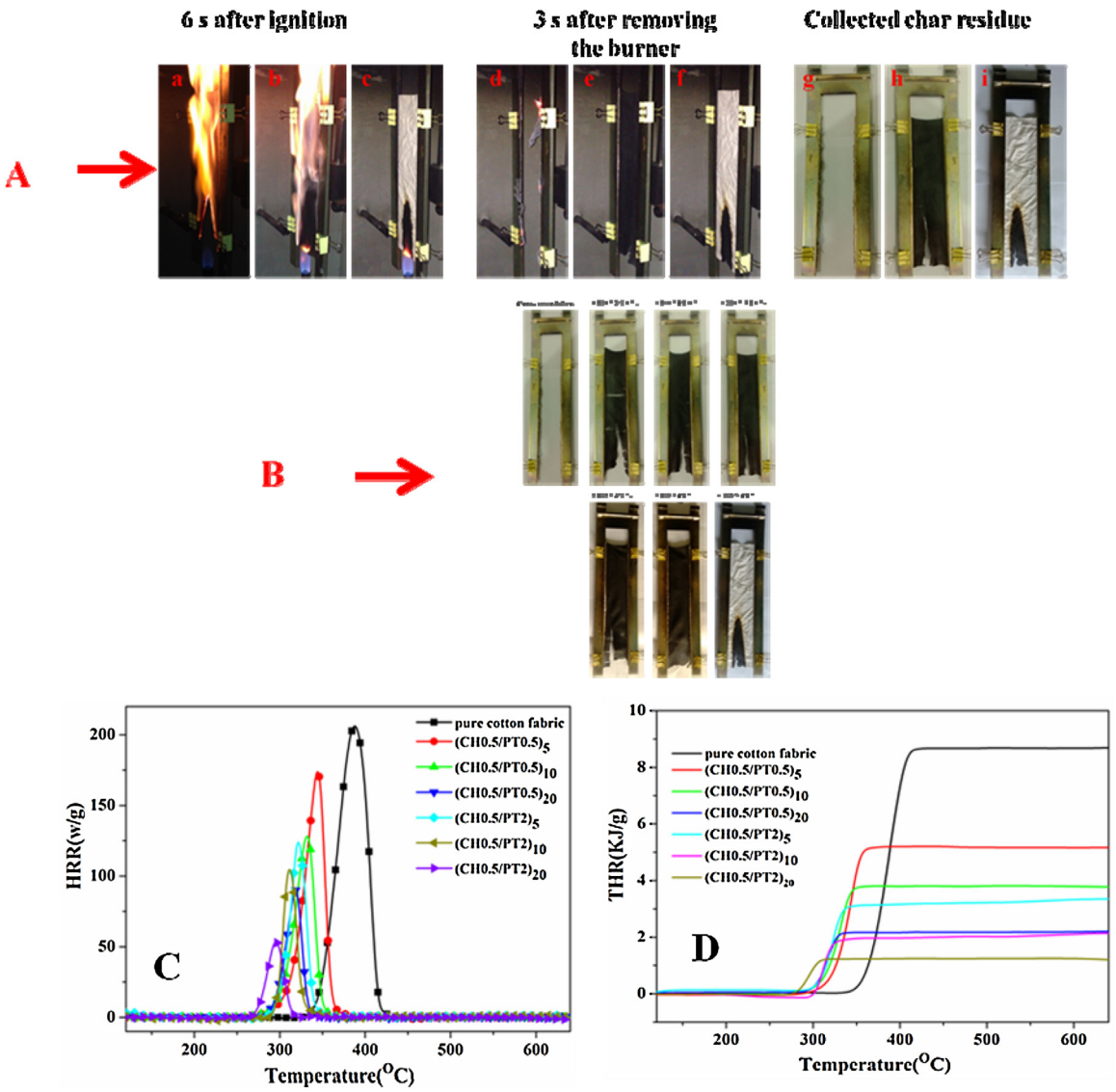

Fig. 3. (A) Real-time images of vertical flame tests for (a, d, g) pristine cotton fabric, (b, e, h) $(CH0.5/PT0.5)_{20}$ and (c, f, i) $(CH0.5/PT2)_{20}$, respectively; (B) Images of pure and (CH/PT) coated cotton fabrics after vertical flame test; Heat release rate (C) and total heat release (D) as a function of temperature for pure and (CH/PT) coated cotton fabrics;.

participate in the charring process, rather than transferred into the MCC combustor (Lu et al., 2011).

10. The analysis of real-time Fourier transform infrared spectra (RT-IR)

In order to further investigate the thermal degradation of coated cotton fabrics. The pure cotton fabric and $(CH0.5/PT2)_{20}$ sample are chosen to measure the change in spectra of real-time FTIR, as shown in Fig. 4. It can be found that characteristic peaks of pure cotton fabric do not change except the peak at 1635 cm^{-1}, which is corresponding to the stretching vibration of H—O—H of physical absorbed water. The peak is disappeared at around 200 °C. The absorptions at 3400 cm^{-1} (stretching vibration of O—H), 2905 cm^{-1}(stretching vibration of C—H), 1435 cm^{-1} (in plane bending vibration of C—H) and 1046 cm^{-1} (stretching vibration of C—O—C) disappear at 300 °C, indicating that cotton fabric decompose and carry on the dehydration reaction of cellulose chain. At the same time, some new peaks at 1710 cm^{-1}, 1443 cm^{-1} (stretching vibration of C=O) and 1613 cm^{-1} (stretching vibration of C=C) appear above 300 °C, further indicating the happen of hydration reaction of cellulose chain and producing aldehydes, ketones and other olefin compounds. However, with further increasing temperature, the relative intensity of the absorption peaks (the absorptions of C=O) continues to weaken until disappear, which indicates that the system is carrying out decarboxylation reaction and producing combustible gasses like aldehydes, ketones, etc. All peaks almost disappear at 500 °C except the absorption at 1443 cm^{-1} (condensed aromatics), indicating that pure cotton fabric decomposes completely and forms the comparatively stable char layer.

As for $(CH0.5/PT2)_{20}$ sample, some different thermal decomposition can be observed. The absorption at 3400 cm^{-1} disappears earlier compared with pure cotton fabric, indicating coated cotton fabric could carry out the dehydration reaction early, which is consistent with the TGA result. The peak at 1060 cm^{-1} (stretching vibration of P—O—C) vanished at 240 °C, implying the breaking of P—O—C structure. The new peaks at 1098 and 870 cm^{-1} (the symmetric and asymmetric stretching vibration of P—O—P band) (Bugajn & Bourbigot, 1999) appear above 300 °C, indicating the formation of poly phosphoric acid (PPA). Meanwhile, a new peak at 1280 cm^{-1}(stretching vibration of P=O) appear (Zhu & Shi, 2003). It indicates that the phosphate group deviates from the aliphatic structure and then forms PPA or re-links to the aromatic

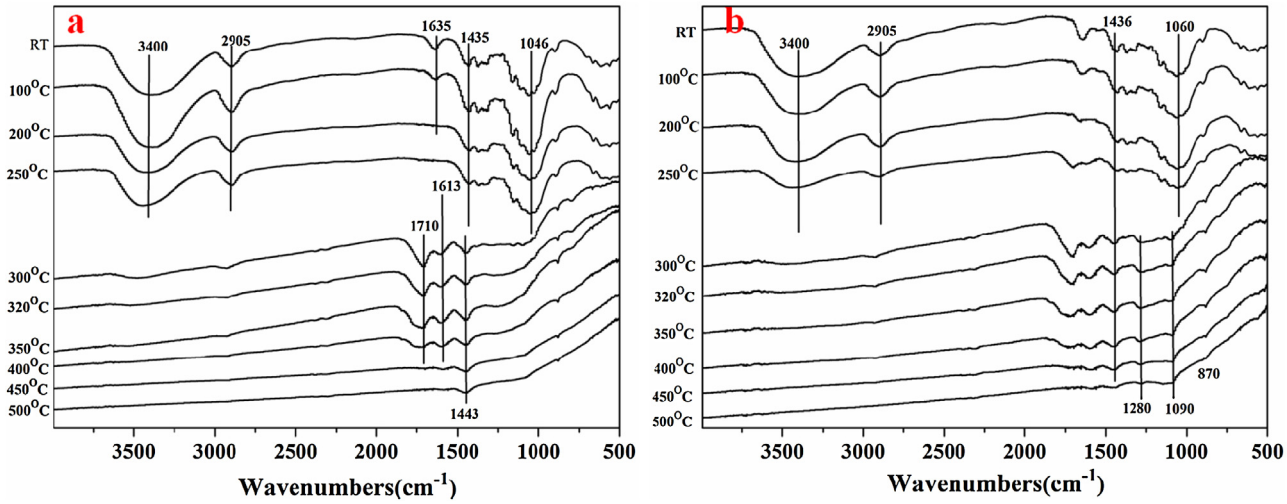

Fig. 4. Real-FTIR Spectra of pure cotton fabric (A) and $(CH0.5/PT2)_{20}$ sample (B) at different degradation temperatures.

structures at the temperatures over 300 °C. Furthermore, the peaks at 1280 cm^{-1}, 1090 cm^{-1} and 870 cm^{-1} are still obvious indicating that the char contained complex P—O—P and P—O—Φ structures, which show compact char structure with high thermal stability (Bourbigot, Bras, & Duquesne, 2004).

11. Volatilized products analysis of pure and coated cotton fabrics

Thermogravimetric analysis/infrared spectrometry (TGA-IR) was performed to analyze the volatilized products after thermal decomposition of samples, which contributed to study the thermal degradation process.

Fig. 5 shows the main absorbance of pyrolysis products for pure cotton fabric and $(CH0.5/PT2)_{20}$ sample. The data obtained from pure cotton fabric and $(CH0.5/PT2)_{20}$ sample can be compared quantitatively as the weight of sample during the testing of each sample is kept constant (1 mg). Total and some specific volatilized products were chosen to study, concluding H_2O (3575 cm^{-1}), hydrocarbons (2820 cm^{-1}), CO_2 (2360 cm^{-1}), CO (2180 cm^{-1}), carbonyl compounds (1741 m^{-1}) and CH_3OH (1100 cm^{-1}). As shown in Fig. 5, it can be found that the released peak of $(CH0.5/PT2)_{20}$ sample appears at 15 min, which is 3 min earlier than that of pure cotton fabric. It indicates that phosphorus-containing Layer-by-Layer nanocoating promotes thermal degradation of cotton fabric at a lower temperature. Therefore, the volatilized products come up earlier. Additionally, the absorption intensity of volatilized products for $(CH0.5/PT2)_{20}$ sample is lower than that for pure cotton fabric, especially for CO and CH_3OH. TGA curves have proved that $(CH0.5/PT2)_{20}$ sample has higher char residue, which is usually used as physical protective barrier to restrain the transfer of mass and heat and insulate oxygen. So, the absorption intensity of flammable volatilized products for $(CH0.5/PT2)_{20}$ sample decreased extraordinarily compared with pure cotton fabric. Therefore, it will be beneficial for fire rescue when an accident happens.

12. Analysis of the collected char residues

In an effort to understand the burn behavior of coated cotton fabrics better, the char residues of (CH0.5/PT2) coated cotton fabrics after vertical flame tests were collected and analyzed by SEM as shown in Fig. 6A. All (CH0.5/PT2) coated cotton fabrics

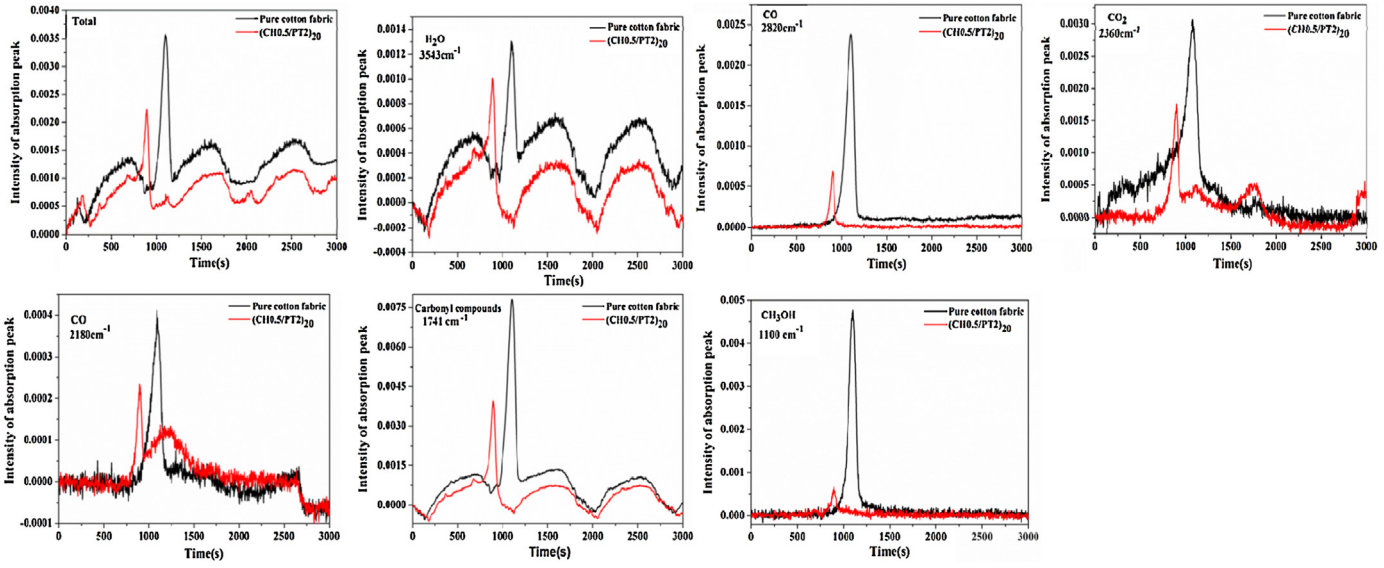

Fig. 5. Absorbance of pyrolysis products for pure cotton fabric and $(CH0.5/PT2)_{20}$ sample.

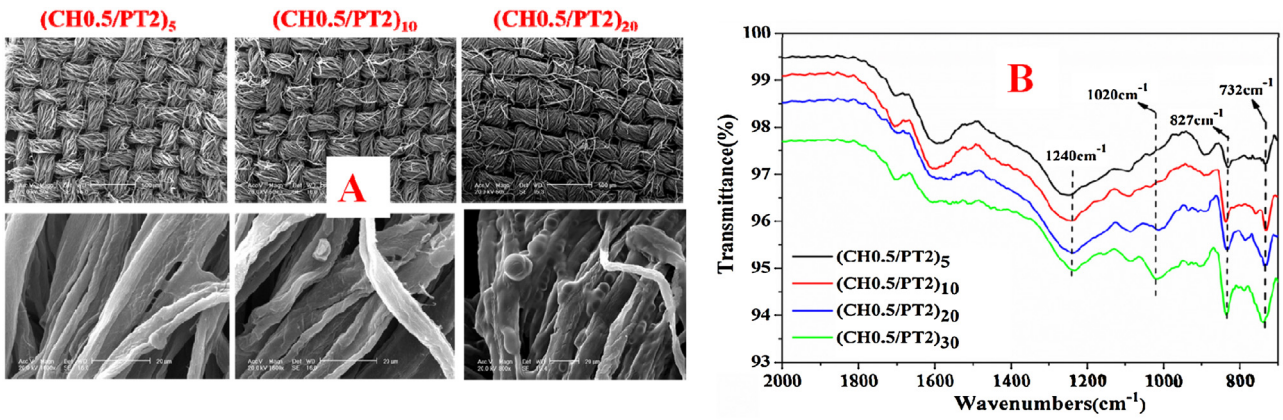

Fig. 6. (A) SEM images and of pure and (CH0.5/PT2) coated cotton fabrics after the vertical flame test; (B) ATR-FTIR spectra of residual char of (CH0.5/PT2) coated cotton fabrics after vertical flame test.

can retain the orthogonal plain-weave architecture and no shrinkage is observed after burning. At low magnification, when bilayers number is increased from 5 to 20, the density of weave structure of residues becomes compact. It indicates that more PT content for coated cotton fabric is contributed to retain the virgin structure of fibers by the protective effect of enough char residue. At high magnification, different morphologies of coated cotton fabrics with different bilayers can be observed. For $(CH0.5/PT2)_5$ and $(CH0.5/PT2)_{10}$ samples, fibers still have the same shape and size, which is similar to the structure of fibers before burning. However, some different images can be observed for $(CH0.5/PT2)_{20}$ samples. The interspaces between fibers associated with the surface are filled up with some small-sized bubbles, which are demonstrating excellent intumescent effect (Laufer et al., 2012; Li et al., 2011; Li et al. 2011a, 2011b). The intumescent char can insulate the heat transformation and the dispersion of oxygen into underlying polymeric substrate to prevent thermo-oxidative reactions.

In order to understand the composition and content of coated cotton fabric surface after the vertical flame test, ATR-FTIR spectra of char residue for (CH0.5/PT2) coated cotton fabrics were analyzed. As shown in Fig. 6B, the peak at 1580 cm^{-1} reveals the formation of an aromatic carbonaceous structure (Sevilla & Fuertes, 2009), peaks at 1090 cm^{-1}, 827 cm^{-1} (stretching vibration of P—O—P) and 1240 cm^{-1}(stretching vibration of P═O) can be also observed, which is consistent with the real-time FTIR result. In addition, the intensity of those peaks absorbance (1090 cm^{-1}, 827 cm^{-1} and 1240 cm^{-1}) increases obviously as the bilayers' number increases. Combining with the TGA result, it indicates that Layer-by-Layer assembled coating mainly plays the condensed phase flame retardant mechanism role for improving flame retardancy of cotton fabric.

13. Conclusion

In conclusion, this work provided a self-extinguishing intumescent coating consisting of biobased fully chitin derivatives on cotton fabric by the Layer-by-Layer assembled method. By altering the concentration of phosphorylated chitin (PT), it could modify its final PT content on cotton fabrics. As the number of bilayers increased, the P/C and P/O ratio values of the coated cotton fabrics were increased, revealing reproducible coverage of phosphorylated chitin on the surface of cotton fabric. Studies on thermal properties demonstrated that all coated cotton fabrics show higher thermal and thermal oxidation stability than that of pure cotton fabric at the temperatures ranging from 400 to 700 °C. In the vertical flame test, the sample coated with 20 bilayers prepared at high PT concentration (2 wt%) could extinguish the flame, and almost 90% unburned cotton fabric can be preserved. All coated cotton fabrics showed lower PHRR and THR in relative to pure one. The $(CH0.5/PT2)_{20}$ sample showed greatest reduction of PHRR and THR. The RT-IR result of coated cotton fabric indicated the formation of stable char contained complex P—O—P and P—O—Φ structures. As for coated cotton fabrics, released amounts of pyrolysis products such as CO_2, CH_3OH, carbonyl compounds, were lower than that for pure cotton fabric owing to barrier and insulating behavior of phosphorus containing char residue with high thermal stability. SEM images showed that small-sized bubbles were formed on top and in the space between fibers when the sample was coated with 20 bilayers at the higher PT concentration (2 wt%) after the vertical flame test. This work expanded the flame retardant application of chitin derivatives for cotton fabric by a simple and versatile method (Layer-by-Layer self-assembly).

Acknowledgment

The work was financially supported by the National Basic Research Program of China (973 Program) (2012CB719701), National Key Technology R&D Program (2013BAJ01B05), National Natural Science Foundation of China (21374111) and National Natural Science Foundation of China (51303165).

Appendix A. Supplementary data

Supplementary data associated with this article can be found, in the online version, at http://dx.doi.org/10.1016/j.carbpol.2014.08.084.

References

Alongi, J., Carosio, F., & Malucelli, G. (2012). Flammability and combustion properties of ammonium polyphosphate-/poly(acrylic acid)-based layer by layer architectures deposited on cotton, polyester and their blends. *Polymer Degradation and Stability*, *97*, 1644–1653.

Bourbigot, S., Bras, M. L., & Duquesne, S. M. (2004). Rochery, recent advances for intumescent polymers. *Macromolecular Materials and Engineering*, *289*, 499–511.

Bugajn, M., & Bourbigot, S. (1999). The origin and nature of flame retardance in ethylene-vinyl acetate copolymers containing hosta flam AP 750. *Polymer International*, *48*, 264–270.

Carosio, F., Alongi, J., & Malucelli, G. (2011). α-Zirconium phosphate-based nanoarchitectures on polyester fabrics through layer-by-layer assembly. *Journal of Materials Chemistry*, *21*, 10370–10376.

Carosio, F., Laufer, G., Alongi, J., Camino, G., & Grunlan, J. C. (2011). Layer-by-layer assembly of silica-based flame retardant thin film on PET fabric. *Polymer Degradation and Stability*, *96*, 745–750.

Carosio, F., Alongia, J., & Malucelli, G. (2012). Layer by layer ammonium polyphosphate-based coatings for flame retardancy of polyester–cotton blends. *Carbohydrate Polymers*, *88*, 1460–1469.

Carosio, F., Blasio, A. D., Alongi, J., & Malucelli, G. (2013). Green DNA-based flame retardant coatings assembled through layer by layer. *Polymer*, *54*, 5148–5153.

Gorochovceva, N., & Makusuka, R. (2004). Synthesis and study of water-soluble chitosan-O-poly(ethylene glycol) graft copolymers. *European Polymer Journal*, *40*, 685–691.

Gaan, S., & Sun, G. (2007). Effect of phosphorus and nitrogen on flame retardant cellulose: A study of phosphorus compounds. *Journal of Analytical and Applied Pyrolysis*, *78*, 371–377.

Gaan, S., Rupper, P., & Salimova, V. (2009). Thermal decomposition and burning behavior of cellulose treated with ethyl ester phosphoramidates: Effect of alkyl substituent on nitrogen atom. *Polymer Degradation and Stability*, *94*, 1125–1134.

Giraud, S., Bourbigot, S., & Rochery, M. (2002). Microencapsulation of phosphate: Application to flame retarded coated cotton. *Polymer Degradation and Stability*, *77*, 285–297.

Hu, S., Song, L., Pan, H. F., Hu, Y., & Gong, X. L. (2012). Thermal properties and combustion behaviors of flame retarded epoxy acrylate with a chitosan based flame retardant containing phosphorus and acrylate structure. *Journal of Analytical and Applied Pyrolysis*, *97*, 109–115, 2012

Hu, S., Song, L., Pan, H. F., & Hu, Y. (2012). Thermal properties and combustion behaviors of chitosan based flame retardant combining phosphorus and nickel. *Industrial and Engineering Chemistry Research*, *51*, 3663–3669.

Hu, S., Song, L., Pan, H. F., & Hu, Y. (2013). Effect of a novel chitosan-based flame retardant on thermal and flammability properties of polyvinyl alcohol. *Journal of Thermal Analysis and Calorimetry*, *112*, 859–864.

Horrocks, A. R., Wang, M. Y., & Hall, M. E. (2000). Flame retardant textile back-coatings. Part 2. Effectiveness of phosphorus-containing flame retardants in textile back-coating formulations. *Polymer International*, *49*, 1079–1091.

Horrocks, A. R., Kandola, B. K., & Davies, P. J. (2005). Developments in flame retardant textiles—A review. *Polymer Degradation and Stability*, *88*, 3–12.

Jayakumar, R., Egawa, T., Furuike, T., Nair, S. V., & Tamura, H. (2009). Synthesis, characterization, and thermal properties of phosphorylated chitin for biomedical applications. *Polymer Engineering and Science*, *49*, 844–849.

Jayakumar, R., Prabaharan, M., Reis, R. L., & Mano, J. F. (2005). Aft copolymerized chitosan-present status and applications. *Carbohydrate Polymers*, *62*, 142–215.

Kurita, K. (2001). Controlled functionalization of polysaccharide chitin. *Progress in Polymer Science*, *26*, 1921–1971.

Kim, S. S., Kim, S. H., & Lee, Y. M. (1996). Preparation, characterization, and properties of β chitin and N-acetylated & Chitin. *Journal of Polymer Science: Polymer Physics*, *34*, 2367–2374.

Kandola, B. K., Horrocks, A. R., & Price, D. (1996). Flame-retardant treatments of cellulose and their influence on the mechanism of cellulose pyrolysis. *Journal of Macromolecular Science: Part C*, *36*, 721–794.

Li, Y. C., Schulz, J., & Grunlan, J. C. (2009). Polyelectrolyte/nanosilicate thin-film assemblies: Influence of pH on growth, mechanical behavior, and flammability. *ACS Applied Materials and Interfaces*, *10*, 2338–2347.

Li, Y. C., Mannen, S., Schulz, J., & Grunlan, J. C. (2011). Growth and fire protection behavior of POSS-based multilayer thin films. *Journal of Materials Chemistry*, *21*, 3060–3069.

Li, Y. C., Mannen, S., Morgan, A. B., Chang, S., Yang, Y. H., & Condon, B. (2011). Intumescent all-polymer multilayer nanocoating capable of extinguishing flame on fabric. *Advanced Materials*, *23*, 3926–3931.

Li, Y. C., Mannen, S., Morgan, A. B., Chang, S., & Yang, Y. H. (2011). Flame retardant finishing of nylon/cotton blend fabric using a hydroxy-functional organophosphorus oligomer. *Advanced Materials*, *23*, 3926–3931.

Li, Y. C., Schulz, J., Mannen, S., Delhom, C., Condon, B., & Chang, C. (2010). Flame retardant behavior of polyelectrolyte-clay thin film assemblies on cotton fabric. *ACS Nano*, *4*, 3325–3337.

Lu, H. D., Wilkie, C. A., Ding, M., & Song, L. (2011). Flammability performance of poly(vinyl alcohol) nanocomposites with zirconium phosphate and layered silicates. *Polymer Degradation and Stability*, *96*, 1219–1224.

Laufer, G., Carosio, F., Martinez, R., Camino, G., & Grunlan, J. C. (2011). Growth and fire resistance of colloidal silica-polyelectrolyte thin film assemblies. *Journal of Colloid and Interface Science*, *56*, 69–77.

Laufer, G., Kirkland, C., Morgan, A. B., & Grunlan, J. C. (2012). Intumescent multilayer nanocoating, made with renewable polyelectrolytes, for flame-retardant cotton. *Biomacromolecules*, *13*, 2843–2848.

Marguerite, R. (2006). Chitin and chitosan: Properties and applications. *Progress in Polymer Science*, *31*, 603–632.

Ma, H., Tong, L., Xu, Z., Fang, Z., Jin, Y., & Lu, F. (2007). A novel intumescent flame retardant: Synthesis and application in ABS copolymer. *Polymer Degradation and Stability*, *92*, 720–726.

Nishi, N., Ebina, A., Nishimura, S., Tsutsumi, A., Hasegawa, O., & Tokura, S. (1986). Highly phosphorylated derivatives of chitin, partially deacetylated chitin and chitosan as new functional polymers: Preparation and characterization. *International Journal of Biological Macromolecules*, *8*, 311–317.

Price, D., Horrocks, A. R., & Akalin, M. (1997). Influence of flame retardants on the mechanism of pyrolysis of cotton (cellulose) fabrics in air. *Journal of Analytical and Applied Pyrolysis*, *40*, 511–524.

Shafizadeh, F., & Fu, Y. L. (1973). Pyrolysis of cellulose. *Carbohydrate Research*, *29*, 113–122.

Sevilla, M., & Fuertes, A. B. (2009). The production of carbon materials by hydrothermal carbonization of cellulose. *Carbon*, *9*, 2281–2289.

Wang, X. H., Zhu, Y., Feng, Q. L., Cui, F. Z., & Ma, J. B. (2003). Responses of osteo- and fibroblast cells to phosphorylated chitin. *Journal of Bioactive and Compatible Polymers*, *18*, 135–146.

Wang, X., Ma, J., Wang, Y., & He, B. (2002). Bone repair in radii and tibias of rabbits with phosphorylated chitosan reinforced calcium phosphate cements. *Biomaterials*, *23*, 4167–4176.

Wang, X., Ma, J., Feng, Q. L., & Cui, F. Z. (2002). Skeletal repair in rabbits with calcium phosphate cements incorporated phosphorylated chitin. *Biomaterials*, *23*, 4591–4600.

Yang, Z., Wang, X., Lei, D., Fei, B., & Xin, J. H. (2012). A durable flame retardant for cellulosic fabrics. *Polymer Degradation and Stability*, *97*, 2467–2472.

Yui, T., Kobayashi, H., Kitamura, S., & Imada, K. (1994). Conformational analysis of chitobiose and chitosan. *Biopolymers*, *34*, 203–207.

Yoshifuji, A., Noishiki, Y., Wada, M., Heux, L., & Kuga, S. (2006). Esterification of β-chitin via intercalation by carboxylic anhydrides. *Biomacromolecules*, *7*, 2878–2881.

Yokogawa, Y., Paz Reyes, J., Mucalo, M. R., Toriyama, M., Kawamoto, Y., Suzuki, T., et al. (1997). Growth of calcium phosphate on phosphorylated chitin fibres. *Journal of Materials Science: Materials in Medicine*, *8*, 407–412.

Zhang, M., & Ren, H. X. (2007). Structural modification and application of chitosan. *Journal of Clinical Rehabilitative Tissue Engineering Research*, *11*, 9817–9820.

Zhang, T., Yan, H. Q., Peng, M., Wang, L. L., Ding, H. L., & Fang, Z. P. (2013). Construction of flame retardant nanocoating on ramie fabric via layer-by-layer assembly of carbon nanotube and ammonium polyphosphate. *Nanoscale*, *5*, 3013–3021.

Zhang, T., Yan, H. Q., Wang, L. L., & Fang, Z. P. (2013). Controlled formation of self-extinguishing intumescent coating on ramie fabric via layer-by-layer assembly. *Industrial and Engineering Chemistry Research*, *52*, 6138–6614.

Zhu, S. W., & Shi, W. F. (2003). Thermal degradation of a new flame retardant phosphate methacrylate polymer. *Polymer Degradation and Stability*, *80*, 217–222.